RESEARCH PAPER

# Thermodynamic Modeling of the Gas-Antisolvent (GAS) Process for Precipitation of Finasteride

**Mohammad Najafi, Nadia Esfandiari\*, Bizhan Honarvar, Zahra Arab Aboosadi**

Department of Chemical Engineering, Marvdasht Branch, Islamic Azad University, Marvdasht, Iran

## Abstract

Experimental study of the effect of gas antisolvent (GAS) system conditions on the particle size distribution of finasteride (FNS) requires a thermodynamic model for the volume expansion process. In this study, the phase behavior of the binary system including carbon dioxide and Dimethyl sulfoxide, and a ternary system comprising carbon dioxide, dimethyl sulfoxide, and Finasteride was studied. The Peng-Robinson equation of state was employed for the evaluation of the fluid phases and a fugacity expression to represent the solid phase. By developing an accurate predictive model, the GAS operating conditions can be optimized to produce particles with no need for a large number of experiments. First, the critical properties of the FNS were evaluated by the group contribution methods. The method of Marrero and Gani was also selected to predict the normal boiling point, critical temperature, and critical pressure. The correlation of Edmister was chosen for the prediction of the acentric factor. The lowest pressures for the ternary system at 308, 318, 328, and 338 K were 7.49, 8.13, 8.51, and 9.03 MPa, respectively. The precipitation of the dissolved finasteride happened at these operating pressures.

## Introduction

The processes of preparing pharmaceutical products require the generation of very small and pure drug particles. The use of small particles in the drug delivery applications will decline the number of required particles [1-4]. Recently, supercritical fluids (in particular, carbon dioxide) have been used for processing pharmaceutical particles through different techniques, such as rapid expansion of supercritical solutions (RESS), gas antisolvent precipitation (GAS), solution enhanced dispersion by SCF (SEDS), supercritical antisolvent methods (SAS), and aerosol supercritical extraction system (ASES) [5-8]. Supercritical carbon dioxide (SC-$CO_2$) could act as either a solvent or an anti-solvent. SC-$CO_2$ has been studied as a suitable alternative to conventional solvents that may damage sensitive compounds like pharmaceuticals. It has low critical temperature and pressure (Tc = 304.2K and Pc = 7.38MPa, respectively). SC-$CO_2$ offers additional benefits due to its nontoxicity, cost-effectiveness, nonflammability, and environmental-friendliness [5,9-12]. The gas anti-solvent (GAS) system can resolve the problem of the low solubility of most substances, especially pharmaceuticals, in supercritical fluids. The gas anti-solvent process has three components: i) a low-volatile organic solvent, ii) a highly volatile anti-solvent, and iii) a solute. The solute and anti-solvent must have a definite level of solubility in the solvent. In the GAS process, a solid dissolved in an organic solvent and a high-pressure gas (in particular, carbon dioxide ($CO_2$) at a given temperature and pressure) are injected into the liquid-phase solution [13-17]. Submicron particle sizes have been obtained using the GAS process from various drugs such as mefenamic acid-nicotinamide

\* Corresponding author:
Email: esfandiari_n@miau.ac.ir (N. Esfandiari)

(MEF-NIC) cocrystal [18], paracetamol into silica aerogel [19], mefenamic acid (MEF) and polyvinylpyrrolidone (PVP) [20], ibuprofen with (R)-phenylethylamine [21] and 5-Fluorouracil [22]. In this process, the solubility of carbon dioxide as an anti-solvent gas is very high in the liquid solvent and may cause a volume expansion in the liquid solvent. Therefore, the solute solubility in the expanded liquid phase reduces by carbon dioxide. As a result, the precipitation of the dissolved compound will occur giving a rise to small particles with a fine size distribution.

In the gas anti-solvent system, process variables, such as temperature, pressure, and solute initial concentration can dramatically influence the morphology of the particles, as well as their particle size and particle size distribution [5,16,22-28].

For evaluation of the appropriate operating conditions for such a process and optimizing the effective parameters, it is necessary to know the thermodynamic model of the volume expansion in the GAS process before performing any experiments [29,30].

The most accurate EoS (presented by De la Fuente Badila et al. [27]) was employed to estimate the relative molar volume variations. For example, Esfandiari et al. [31] optimized for a binary (DMSO-$CO_2$) and a ternary (DMSO–$CO_2$-ampicillin) system. The thermodynamic modeling was conducted based on the Peng-Robinson equation of state with a linear combination of Vidal and Michelsen mixing rules (PR-LCVM). The optimal condition for ampicillin precipitation was determined through modeling the volume expansion and phase equilibrium. Optimum conditions were investigated for binary systems of $CO_2$-diethyl succinate and $CO_2$-ethyl acetate as well as the ternary systems of $CO_2$-diethyl succinate-ethanol and $CO_2$-diethyl succinate-ethyl acetate [32].

Moreover, Sue et al. [33] employed volume-translated Peng-Robinson (VTPR) to assess the total volume expansion of DMSO and $CO_2$. To this end, the relative molar volume variation was evaluated in terms of pressure using VTPR-EoS. The minimum pressure at 308.15 K was determined to be 7.65 MPa.

Finasteride is a 5α-reductase inhibitor. It is specifically a selective inhibitor of type II and III isoforms of the enzyme. It has been applied for the treatment of benign prostatic hyperplasia (BPH) symptoms in men with prostate enlargement, prostate cancer, and androgenetic alopecia. This drug was used to stimulate hair growth in men with mild to moderate androgenic alopecia (male pattern alopecia, hereditary alopecia, common male baldness) [34,35].

Following biopharmaceutical classification, finasteride (FNS) is a member of class 2 drugs with high permeability and poor solubility in water. Its water solubility was reported to be 0.05 mg/ml at the pH range of 1 to 13 which is very low. It is a weakly acidic drug with pKa of 15.9 [34]. FNS is also poorly soluble in supercritical carbon dioxide (molar fraction solubility $10^{-5}$ to $10^{-4}$ at $308 \leq T \leq 348$ K and $121 \leq P \leq 355$ bar) [36].

This work is aimed to study the phase behavior of binary (DMSO-$CO_2$) and ternary ($CO_2$ +DSMO+Finasteride) systems. The Peng-Robinson equation of state (EoS) with vdW2 mixing rules was also used to represent the fluid phases and the fugacity of the precipitated solid phase. The volume expansion and phase equilibrium were also modeled to optimize the condition for finasteride precipitation.

## Thermodynamic Framework

Thermodynamic studies in gas-liquid systems are often difficult for products that are distributed between the liquid and the vapor phase. Therefore, the description of the phase equilibrium is usually performed by an equation of state (EoS). Usually, cubic equations of state are used to develop the methods for estimating the vapor-liquid thermodynamic equilibrium. Furthermore, the equation of states should be modified to evaluate the fractions of the liquid and vapor phases in the mixture of hydrocarbons. In the GAS systems, high-pressure $CO_2$ is injected into the

solution, which will cause a volume expansion in the solution giving rise to the particle precipitation in a short period. In this regard, the optimal conditions of finasteride were calculated for binary ($CO_2$-DMSO) and ternary (DMSO-$CO_2$-finasteride) systems. For this purpose, VLE data were modeled via the Peng-Robinson equation of state with van Der Waals Mixed Rules (vdW2) before the experiments. In the modeling of the GAS process, the pressure and temperature of all phases are assumed equal. Additionally, due to the low volume of precipitator and mixing of liquid and gas phases, mass transfer resistance is not considered [27,31,37,38].

### Binary System Anti-Solvent (1)-Solvent (2)

As the classical liquid-phase volume expansion is given for the determination of a proper solvent and operation conditions, De la Fuente Badilla et al. [39] represented that the use of the relative molar volume changes of the liquid phase is more convenient for optimization of the GAS process condition. Therefore, the following definition can be presented for the relative molar volume change [31,37,39,40]:

$$\frac{\Delta V}{V} = \frac{V_L(T.\ P) - V_2(T.\ P_0)}{V_2(T.\ P_0)} \tag{1}$$

Eq. 1 only represents the relationship between molar volumes of the liquid phase in the mixture and the pure solvent. In Eq. 1, $V_2(T.\ P_0)$ demonstrates the molar volume of a pure solvent at the system temperature and reference pressure (usually at 101.325 KPa), while $V_L(T.\ P, X_1)$ stands for the molar volume of the liquid phase at a given temperature and the pressure of the binary mixture, and $X_1$ represents the mole fraction of $CO_2$ dissolved in the liquid phase.

### Ternary Systems Anti-Solvent (1)-Solvent (2)-Solute (3)

In this research, the methods presented by De la Badilla et al. [39], and Shariati and Peters [37] were proposed for modeling. The equilibrium criteria for the solid-liquid-vapor three-phase equilibria implies equal temperature, pressure, and fugacity of components ($CO_2$, DMSO, and finasteride) in the three possible phases. Therefore, the equilibrium criteria for the anti-solvent (1)-solvent (2)-solute (3) can be written as:

$$\frac{\hat{\varphi}_1^L}{\hat{\varphi}_1^V} x_1 - y_1 = 0 \tag{2}$$

$$\frac{\hat{\varphi}_2^L}{\hat{\varphi}_2^V} x_2 - y_2 = 0 \tag{3}$$

$$\frac{\hat{\varphi}_3^L}{\hat{\varphi}_3^V} x_3 - y_3 = 0 \tag{4}$$

$$k_i = \frac{y_i}{x_i} = \frac{\hat{\varphi}_i^v}{\hat{\varphi}_i^L} \tag{5}$$

Eqs. 2 to 4 represent the equilibrium condition for the three phases of liquid, and gas in the GAS process. Eqs. 2 and 3 express the liquid-vapor equilibrium conditions for the two-phase system, while the liquid-vapor equilibrium conditions of the three-phase system are presented in Eqs. 2 to 4. Some assumptions for solid-liquid equilibrium needed during the calculations are [28,36]:

(1) solubility of solvent in the solid phase was negligible,
(2) solubility of anti-solvent in the solid phase was negligible, and
(3) the solid phase was the pure solute.

Using this assumption, Eq. 6 can be derived.

$$\frac{\varphi_3^S}{\hat{\varphi}_3^L}--x_3 = 0 \tag{6}$$

In Eq. 6, $\varphi_3^S$ demonstrates the solute fugacity coefficient in the solid phase. The next limitations were applied for liquid and vapor phases [39,40].

$$\sum_{i=1}^{3} x_i - 1 = 0 \tag{7}$$

$$\sum_{i=1}^{3} y_i - 1 = 0 \tag{8}$$

Eqs. 2 to 7 indicate a set of six equations with six unknown components in the fluid phases in a certain temperature and pressure. For the description of the fluid phases, the Peng-Robenson equation of state is expressed by [37,41]:

$$P = \frac{RT}{v-b} - \frac{a(T)}{v(v+b)+b(v-b)} \tag{9}$$

where $v$ is the molar volume. The quadratic mixing rules in mole fraction for $a$ and $b$ are used as follows:

$$a = \sum_j \sum_i x_i x_j a_{ij} \tag{10}$$
$$b = \sum_j \sum_i x_i x_j b_{ij} \tag{11}$$

where $j$ and $b_{ij}$ are the cross energetic parameter and the cross-co-volume parameter, respectively. $a_{ij}$ and $b_{ij}$ are calculated as follows:

$$a_{ij} = (a_i a_j)^{0.5}(1-k_{ij}) \tag{12}$$
$$b_{ij} = (\frac{b_i+b_j}{2})(1-l_{ij}) \tag{13}$$

In Eqs. 12 and 13, $k_{ij}$ and $l_{ij}$ are the interaction parameters; while $a_i$s and $b_i$s can be given by the following equations:

$$a = 0.45724(\frac{R^2(T_c)^2}{P_c})\alpha(T) \tag{14}$$
$$b = 0.0778\frac{RT_c}{P_c} \tag{15}$$

The temperature-dependent energetic parameter, $\alpha(T)$, can be given by the following equations:

$$\alpha^{1/2} = 1 + k(1-T_r^{1/2}) \tag{16}$$
$$k = 0.37464 + 1.54226\omega - 0.26992\omega^2 \tag{17}$$

where $k$ and $\omega$ are the pure compound parameters of the component $i$, and the acentric factor of the solid compound, respectively. In this study, the phase equilibrium was modeled by the Peng-Robinson equation of state (PR-EoS) with vdW2 mixing rules. By applying thermodynamic manipulations, analytical equations can be obtained from the fugacity of the fluid phases. As the Peng-Robinson EoS fails to show the behaviour of the solid phase, another definition has to be applied for the fugacity of the solid solute [31,37]. The solid phase fugacity coefficient can be defined by the following equation [40]:

$$ln\varphi_3^S = ln\varphi_3^L + \frac{\Delta H_{tp}}{R}(\frac{1}{T_{tp}} - \frac{1}{T}) + \frac{v_{tp}}{RT}(P-P_{tp}) \tag{18}$$

where, $ln\varphi_3^l$ shows the fugacity coefficient of the pure solute in the sub-cooled liquid phase at the temperature $T$, and pressure $P$. $T_{tp}$, $P_{tp}$, $v_{tp}$, and $\Delta H_{tp}$ are triple point temperature, triple point pressure, solute molar volume at the triple point, and heat of fusion at the triple point, respectively. These parameters are necessary for the calculation of the fugacity coefficient of the pure solid phase. The physical properties of finasteride used for the solid phase fugacity evaluation were also calculated. In the present study, the method of Marrero and Gani was proposed for calculating the finasteride properties.

**Genetic Algorithm**

The genetic algorithm (GA) is a meta-heuristic method inspired by the efficiency of natural selection in biological evolution. The genetic algorithm has shown promising potential in various applications. It demonstrates a powerful problem-solving ability that can be successfully applied to a wide variety of complex combinatorial problems. GAs are global search methods made of a few principles like selection, crossover, and mutation. Briefly, GA involves a randomly-generated initial population, a fitness function, and the development of new generations via the application of genetic operators, namely selection, crossover, and mutation [42-44].

In the present work, an effective algorithm was proposed based on a genetic algorithm (GA) technology to efficiently estimate the adjustable parameter of the thermodynamic model. Moreover, finding the global optimum with high probability and significance is not sensitive to the initial estimates of the unknown parameters and the tuning parameters of the model. It was used to select the optimal binary interactive parameters of the PR model. The binary interaction parameters $k_{ij}$ and $l_{ij}$, present in Eqs. 12 and 13, have been optimized using $|\Delta k_i| < \varepsilon$ in this work for each temperature [31].

## Results and discussion

The van der Waals mixing rules with two parameters (vdW2) was applied in this work for mixture calculations. The fluid phase behavior of the binary and ternary systems (DMSO-$CO_2$ and DMSO-$CO_2$ -finasteride) was predicted by the Peng-Robinson equation of state. The first step in the calculation of the phase equilibrium data using the PR EoS is the estimation of boiling point, critical properties, and acentric factor of the drug compounds which can't be measured experimentally. For heavier hydrocarbons, the critical thermodynamic properties are not available at all. Therefore, empirical methods such as group contribution methods or molecular level simulation are often used to evaluate these critical parameters [45,46]. In this research, a group contribution method proposed by Marrero and Gani [47] (considering 182 functional groups) was used to estimate the finasteride properties. In this method, the structure of the compound is determined and the molecules of a compound are collected from different groups. These groups are first-order groups, second-order groups, and third-order groups. The distribution and population of each group are determined. The first-order groups are described as a wide variety of organic compounds. The second and third-order groups are used to describe the molecular structure of compounds. Therefore, the property calculation is performed at three levels. The initial approximation is determined by the first level. Then, the second and third levels refined the initial approximation. The function of property-estimation is given by the following equation:

$$f(X) = \sum_i N_i C_i + w \sum_j M_j D_j + z \sum_k O_k E_k \tag{19}$$

where $C_i$ is the contribution of the first-order group of type-i that happens $N_i$ times, $D_j$ is the contribution of the second-order group of type-j that happens $M_j$ times, and $E_k$ is the contribution of the third-order group of type-k that occurs $Q_k$ times in a compound [48]. The correlation of Edmister was chosen for the prediction of the acentric factor. The critical properties and the acentric factors of FNS, DMSO, and $CO_2$ are listed in Table 1. Furthermore, the physical properties of FNS needed in Eq. 18 are listed in Table 2.

**Table 1.** Critical properties and acentric factor of substances

| Substance | Tc (K) | Pc (bar) | $\omega$ | Ref. |
|---|---|---|---|---|
| $CO_2$ | 304.13 | 73.8 | 0.224 | [46] |
| DMSO | 706.9 | 58.5 | 0.45 | [46] |
| FNS | 902.22 | 16 | 0.42 | This work |

**Table 2.** The physical properties of FNS required in Eq. 17

| Substance | $T_{tp}$ (K) | $P_{tp}$ (pa) | $v_{tp}$ (cm$^3$ mol$^{-1}$) | $\Delta H_{tp}$ (kJ mol$^{-1}$) |
|---|---|---|---|---|
| FNS | 530.85 | 8E+3 | 397.7 | 165.84 |

## Binary System

By defining the molar volume of the liquid solution, the best combination of DMSO and $CO_2$ takes place when a minimum pressure occurs in the volume expansion curve [49,50].

$$v = x_1\bar{v}_1 + x_2\bar{v}_2 \tag{20}$$

In Eq. 20, $v$ is the molar volume of solution, $x_1$ shows the mole fraction of $CO_2$ in the liquid phase, $\bar{v}_1$ represents the partial molar volume of $CO_2$, $x_2$ denotes the mole fraction of the solvent in the liquid phase, and $\bar{v}_2$ stands for the partial molar volume of the solvent. According to Eq. 18 and the relative variation in molar volume-pressure curve, three interesting phenomena can be observed at any temperature: i) with increasing $CO_2$ mole fraction ($x_1$), liquid molar volume ($v$) decreases when ($\bar{v}_1 < \bar{v}_2$), ii) upon an increase in the high value of $CO_2$ mole fraction ($x_1$), liquid molar volume ($v$) reaches a minimum value at $\bar{v}_1 = \bar{v}_2$, and iii) by adding a very high value of $CO_2$ mole fraction ($x_1$), liquid molar volume ($v$) increases for $\bar{v}_1 > \bar{v}_2$ [50]. Fig. 1 shows the variation of the relative molar volume-pressure curve of the liquid phase in the binary system ($CO_2$-DMSO) at 308 K. It is evident that with increasing pressure, a minimum occurred in this curve at 7.27 MPa and a sharp increase of relative variation in molar volume can be observed above this point. Therefore, the optimum pressure for precipitating the solute in the GAS process will be larger than $P_{min}$ (7.27 MPa). The binary interaction parameters $k_{ij}$ and $l_{ij}$, shown in Eqs. 12 and 13, have been optimized using GA for each temperature. Table 3 shows these binary interaction parameters.

Fig. 2 shows the relative changes in the molar volume by variation of the $CO_2$ mole fraction at 308 K. As can be seen, with increasing the $CO_2$ mole fraction, a sharp drop can be detected in relative molar volume change until reaching the lowest value at carbon dioxide mole fraction of 0.714. At this point, by enhancing the $CO_2$ mole fraction of the liquid phase, the variation of relative molar volume showed a vertical increase. According to Figs. 1 and 2, at optimum operational pressure ($P_{min}$ = 7.27 MPa), the $CO_2$ mole fraction is 0.714 in such a way that the change of relative molar volume shows a minimum value.

**Table 3.** Binary interaction parameters from PR and the vdW2 mixing rules for the system $CO_2$ (1) + DMSO (2)
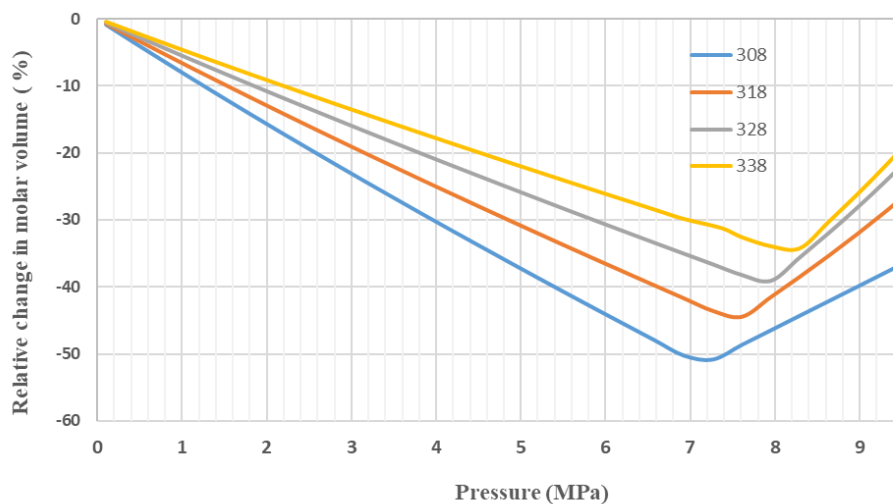
| T (K) | $k_{12}$ | $l_{12}$ |
|---|---|---|
| 308 | 0.035 | 0.031 |
| 318 | 0.026 | 0.016 |
| 328 | 0.019 | 0.011 |
| 338 | 0.011 | 0.007 |
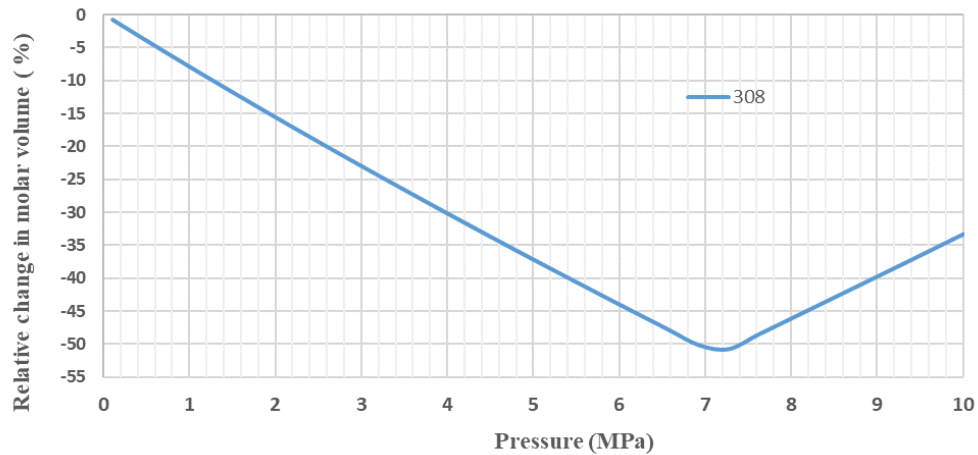
**Fig. 1.** Relative expansion of the liquid phase as a function of pressure, calculated according to PR for the systems DMSO–$CO_2$ at 308 K
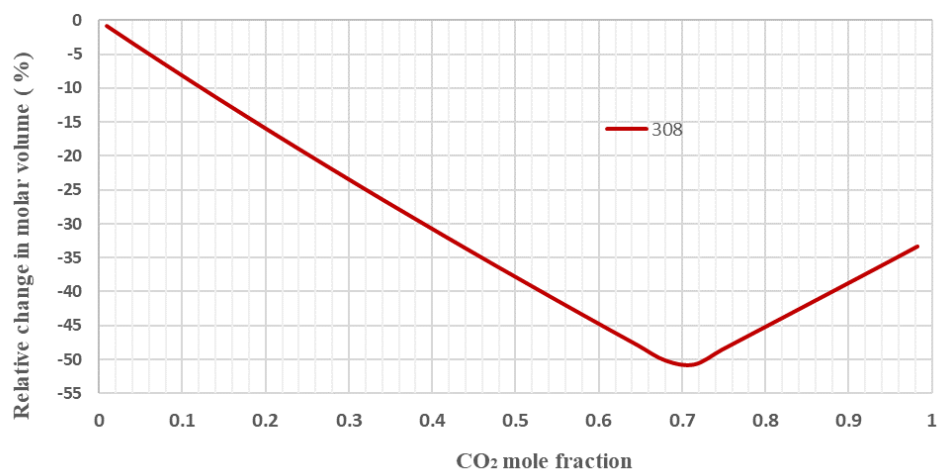


**Fig. 2.** Relative expansion of the liquid phase as a function of $CO_2$ mole fraction in the liquid phase, calculated according to PR for the systems DMSO–$CO_2$ at 308 K



**Fig. 3.** Relative expansion of the liquid phase as a function of pressure, calculated according to PR for the systems DMSO–$CO_2$ at different temperature (308, 318, 328, and 338 K)

Fig. 3 presents the computational results for the binary system (DMSO+$CO_2$) at any temperatures. The minimum pressure showed an increase by temperature enhancement and Pmin was determined 7.27, 7.61, 7.95, and 8.27 MPa at 308, 318, 328, and 338 K, respectively.

Esfandiari et al. [31] calculated the relative variation in molar volume in terms of pressure based on the PR-LCVM equation for the DMSO-$CO_2$ system. The minimum pressure (Pmin) was 7, 7.74, and 8.5 MPa at 308, 313, and 319 K, respectively.

The vapor-liquid equilibrium of DMSO and $CO_2$ as a function of temperature and pressure is presented in Fig. 4. As can be observed, an increase in the pressure and temperature resulted in an increment in the $CO_2$ mole fraction of the liquid phase. The degree of GAS processability to precipitate nanoparticles depended on the extent of mixing of $CO_2$ with solvent. The miscibility of DMSO and $CO_2$ increased with pressure and temperature.

**Ternary System**

The ternary system comprising carbon dioxide-dimethyl sulfoxide–finasteride was studied in this work. The results of finasteride solubility at the liquid phase for this system are shown in Fig. 5. A slight increase can be observed in the finasteride solubility in the liquid phase within a narrow pressure range (~2.4-3.1 MPa) at 308 K. Based on Fig. 5, the minimum pressure in the curve of the finasteride mole fraction in the liquid phase occurred at 7.49 MPa. Also, the binary interaction parameters $k_{ij}$ and $l_{ij}$, for the ternary system shown in Eqs. 11 and 12, have been optimized using GA for each temperature. Table 4 shows these binary interaction parameters.
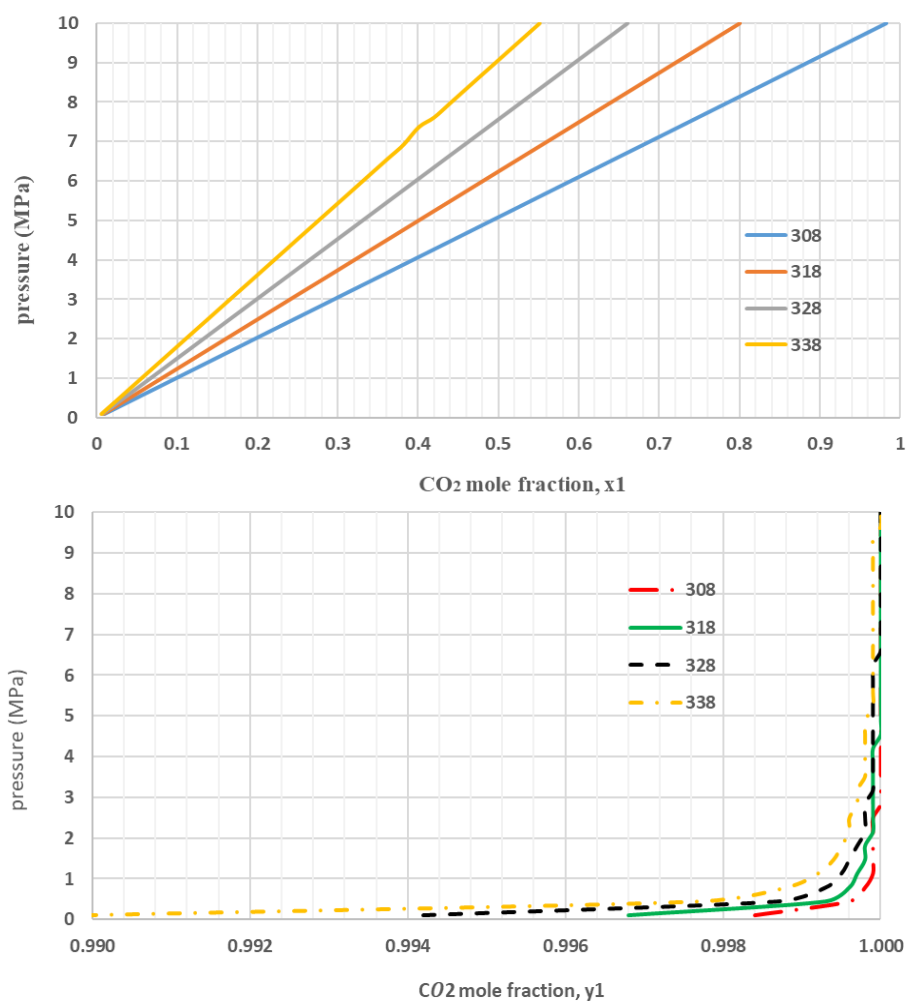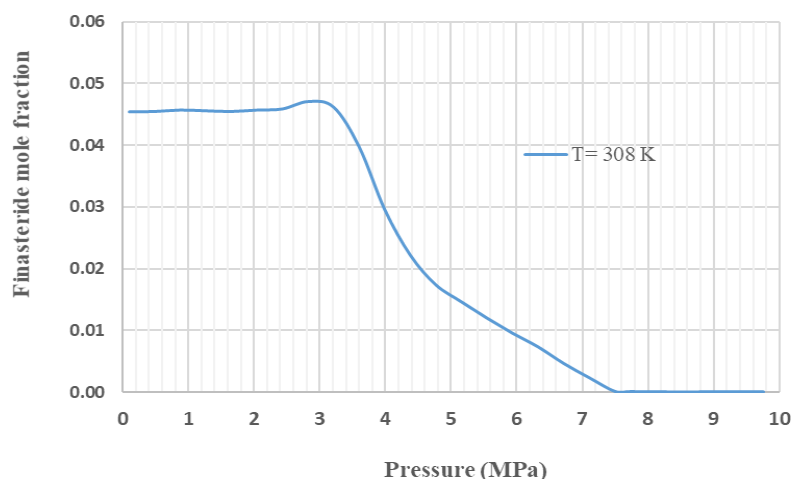


**Fig. 4.** Comparison of VLE of DMSO–$CO_2$ system calculated according to PR at 308, 318, 328, and 338 K

**Fig. 5.** The calculated solubility of FNS in the liquid phase expanded by supercritical $CO_2$ for the ternary system of $CO_2$ -DMSO-finasteride at 308 K

**Table 4.** Binary interaction parameters from PR and the vdW2 mixing rules for the system $CO_2$ (1) + DMSO (2) + FNS (3)

| T (K) | $k_{12}$ | $k_{13}$ | $k_{23}$ | $l_{12}$ | $l_{13}$ | $l_{23}$ |
|---|---|---|---|---|---|---|
| 308 | 0.1950 | 0.2300 | 0.0340 | -0.0230 | 0.0500 | *0.2500* |
| 318 | 0.1190 | 0.2200 | 0.0328 | -0.0240 | 0.0480 | *0.2300* |
| 328 | 0.0930 | 0.2100 | 0.0310 | -0.0250 | 0.0460 | *0.2250* |
| 338 | 0.0900 | 0.1900 | 0.0300 | -0.0260 | 0.0145 | *0.2200* |

Fig. 6 presents the relative molar volume variation of this system at 308 K. As shown in this figure, in the same pressure range a minimum can be detected, showing a sharp decrease in the finasteride concentration. This means that at this point ($P_{min}$ = 7.49 MPa) almost all the solute is precipitated.
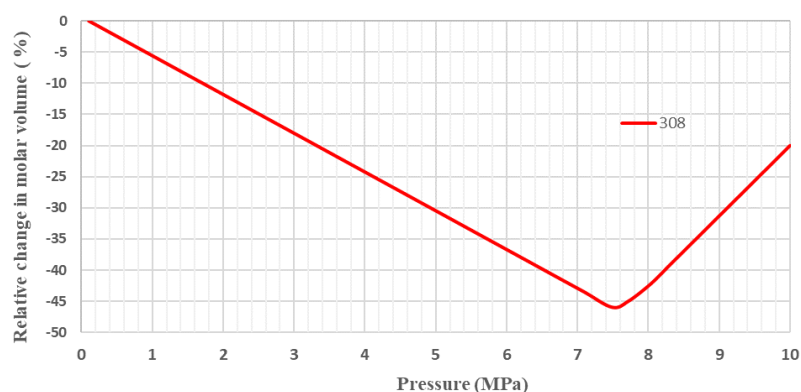


**Fig. 6.** Relative expansion of the liquid phase as a function of pressure, calculated according to PR for the systems DMSO–$CO_2$ –FNS at 308 K

Fig. 7 depicts the relative molar volume change-pressure curve for the ternary system at different temperatures. As can be seen, the minimum value of pressure increased by temperature elevation. The estimated $P_{min}$ were 7.49, 8.13, 8.51, and 9.03 MPa at 308, 318, 328, and 338 K, respectively. The modeling results for the minimum value of pressure in the binary and ternary systems are illustrated in Figs. 3 and 7. Accordingly, the value of $P_{min}$ in the binary system was smaller than that of the ternary system at a constant temperature. This indicates that the optimum operating pressure for the GAS process should be determined in such a way that to show the relative expansion of the liquid phase at least.
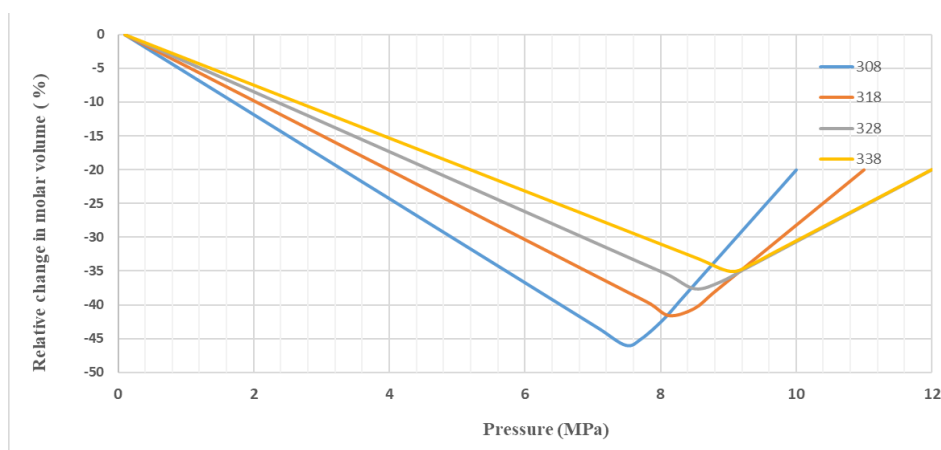
**Fig. 7.** Relative expansion of the liquid phase as a function of pressure, calculated according to PR for the systems $CO_2$ –DMSO–FNS at different temperature (308, 318, 328, and 338 K)

## Conclusion

In this study, the Peng–Robinson equation of state with vdW2 mixing rules was employed to determine the phase equilibrium data for the binary ($CO_2$+DMSO) and ternary ($CO_2$ +DMSO+FNS) systems at temperatures ranging from 308 to 338 K. The method of Marrero and Gani was proposed for calculating the critical properties of the drug. A new explanation of the relative variation in molar volume investigated by De la Fuente Badilla et al. [39] was also adapted for finding the optimum operating condition (T, P) for the GAS process. At certain temperatures, the optimum operating pressure for precipitation of finasteride particles was determined by plotting relative molar volume variation vs. pressure diagrams. This indicates that approximately 100% of FNS particles were precipitated at optimum operating conditions (P, T). The Pmin of the ternary system (DMSO-$CO_2$-FNS) was calculated 7.49, 8.13, 8.51, and 9.03 MPa at 308, 318, 328, and 338 K. By comparing the position of the pressure on the solubility curve of FNS in the liquid phase (Fig. 5) and the relative expansion of the liquid phase (Fig. 6), it can be found that the minimum pressure shown in these figures are the same (Pmin = 7.49 at T = 308 K). Moreover, the results showed that Pmin value increased by temperature enhancement.

## Nomenclature

| | |
|---|---|
| a(T) | Energy parameter of the cubic EoS (J. $m^3$. $mol^{-2}$) |
| b | Volume parameter for equations of state ($m^3$. $mol^{-1}$) |
| $H_{fusion}$ | Heat of fusion for the solute (J. $mol^{-1}$) |
| $k_{ij}$ | Binary interaction parameters in the mixing rules |
| $l_{ij}$ | Binary interaction parameters in the mixing rules |
| P | Pressure (Pa) |
| $P_c$ | Critical pressure (Pa) |
| $P_{ref}$ | Reference pressure (Pa) |
| R | universal Gas constant, R=8.314 (J. $mol^{-1}$. $K^{-1}$) |
| T | Temperature (K) |
| $T_b$ | Boling point temperature (K) |
| $T_c$ | Critical temperature (K) |
| $T_r$ | Reduced temperature |
| v | Molar volume of solution ($m^3$. $mol^{-1}$) |
| $\bar{v}_1$ | Partial molar volume of $CO_2$ ($m^3$. $mol^{-1}$) |
| $\bar{v}_2$ | Partial molar volume of the solvent ($m^3$. $mol^{-1}$) |
| vdW2 | Van der Waals mixing rule with two adjustable parameters |

| $x_i$ | Liquid-phase mole fraction of the component i |
|---|---|
| $y_i$ | Vapor-phase mole fraction of the component i |
| $Z$ | Compressibility factor |

*Greek symbols*

| $\alpha(T)$ | Temperature-dependent equation of state parameter |
|---|---|
| $\Delta$ | Property change |
| $\phi$ | Fugacity coefficient |
| $k$ | Peng-Robinson equation parameter |
| $\omega$ | Acentric factor |

*Subscripts*

| 0 | Reference condition |
|---|---|
| 1 | Anti-solvent |
| 2 | Solvent |
| 3 | Solute |
| c | Critical property |
| i, j | Component |
| L | Liquid phase |
| tp | Triple point |

*Superscripts*

| L | Liquid phase |
|---|---|
| S | Solid-phase |
| V | Vapor phase |

## References

[1] Zodge A, Kőrösi M, Madarász J, Szilágyi IM, Varga E, Székely E. Gas antisolvent fractionation: a new approach for the optical resolution of 4-chloromandelic acid. Periodica Polytechnica Chemical Engineering. 2019 Mar 18;63(2):303-11.

[2] Mihalovits M, Horváth A, Lőrincz L, Székely E, Kemény S. Model Building on selectivity of gas antisolvent fractionation method using the solubility parameter. Periodica Polytechnica Chemical Engineering. 2019 Mar 19;63(2):294-302.

[3] Pessoa AS, Aguiar GP, Oliveira JV, Bortoluzzi AJ, Paulino A, Lanza M. Precipitation of resveratrol-isoniazid and resveratrol-nicotinamide cocrystals by gas antisolvent. The Journal of Supercritical Fluids. 2019 Mar 1;145:93-102.

[4] Gil-Ramírez A, Rodriguez-Meizoso I. Purification of Natural Products by Selective Precipitation Using Supercritical/Gas Antisolvent Techniques (SAS/GAS). Separation & Purification Reviews. 2019 May 23:1-21.

[5] Esfandiari N. Production of micro and nano particles of pharmaceutical by supercritical carbon dioxide. The Journal of Supercritical Fluids. 2015 May 1;100:129-41.

[6] Reverchon E, Adami R. Nanomaterials and supercritical fluids. The Journal of supercritical fluids. 2006 Feb 1;37(1):1-22..

[7] Sodeifian G, Sajadian SA. Solubility measurement and preparation of nanoparticles of an anticancer drug (Letrozole) using rapid expansion of supercritical solutions with solid cosolvent (RESS-SC). The Journal of Supercritical Fluids. 2018 Mar 1;133:239-52.

[8] Bahrami M, Ranjbarian S. Production of micro-and nano-composite particles by supercritical carbon dioxide. The Journal of supercritical fluids. 2007 Mar 1;40(2):263-83.

[9] Sodeifian G, Sajadian SA, Ardestani NS, Razmimanesh F. Production of Loratadine drug nanoparticles using ultrasonic-assisted Rapid expansion of supercritical solution into aqueous solution (US-RESSAS). The Journal of Supercritical Fluids. 2019 May 1;147:241-53.

[10] Sodeifian G, Sajadian SA. Utilization of ultrasonic-assisted RESOLV (US-RESOLV) with polymeric stabilizers for production of amiodarone hydrochloride nanoparticles: Optimization of the process parameters. Chemical Engineering Research and Design. 2019 Feb 1;142:268-84.

[11] Fahim TK, Zaidul IS, Bakar MA, Salim UM, Awang MB, Sahena F, Jalal KC, Sharif KM, Sohrab MH. Particle formation and micronization using non-conventional techniques-review. Chemical Engineering and Processing: Process Intensification. 2014 Dec 1;86:47-52.

[12] Sodeifian G, Sajadian SA, Honarvar B. Mathematical modelling for extraction of oil from Dracocephalum kotschyi seeds in supercritical carbon dioxide. Natural product research. 2018 Apr 3;32(7):795-803.

[13] Kim S, Lee SJ, Seo B, Lee YW, Lee JM. Optimal Design of a Gas Antisolvent Recrystallization Process of Cyclotetramethylenetetranitramine (HMX) with Particle Size Distribution Model. Industrial & Engineering Chemistry Research. 2015 Nov 11;54(44):11087-96.

[14] Kim SJ, Lee BM, Lee BC, Kim HS, Kim H, Lee YW. Recrystallization of cyclotetramethylenetetranitramine (HMX) using gas anti-solvent (GAS) process. The Journal of Supercritical Fluids. 2011 Nov 1;59:108-16.

[15] Foster NR, Kurniawansyah F, Tandya A, Delgado C, Mammucari R. Particle processing by dense gas antisolvent precipitation: ARISE scale-up. Chemical Engineering Journal. 2017 Jan 15;308:535-43.

[16] Jafari D, Yarnezhad I, Nowee SM, Baghban SH. Gas-antisolvent (GAS) crystallization of aspirin using supercritical carbon dioxide: experimental study and characterization. Industrial & Engineering Chemistry Research. 2015 Apr 15;54(14):3685-96.

[17] Park SJ, Yeo SD. Recrystallization of caffeine using gas antisolvent process. The Journal of Supercritical Fluids. 2008 Nov 1;47(1):85-92.

[18] Wichianphong N, Charoenchaitrakool M. Application of Box–Behnken design for processing of mefenamic acid–paracetamol cocrystals using gas anti-solvent (GAS) process. Journal of $CO_2$ Utilization. 2018 Jul 1;26:212-20.

[19] Ulker Z, Erkey C. An advantageous technique to load drugs into aerogels: Gas antisolvent crystallization inside the pores. The Journal of Supercritical Fluids. 2017 Feb 1;120:310-9.

[20] Dittanet P, Phothipanyakun S, Charoenchaitrakool M. Co-precipitation of mefenamic acid−polyvinylpyrrolidone K30 composites using Gas Anti-Solvent. Journal of the Taiwan Institute of Chemical Engineers. 2016 Jun 1;63:17-24.

[21] Lőrincz L, Bánsághi G, Zsemberi M, de Simón Brezmes S, Szilágyi IM, Madarász J, Sohajda T, Székely E. Diastereomeric salt precipitation based resolution of ibuprofen by gas antisolvent method. The Journal of Supercritical Fluids. 2016 Dec 1;118:48-53.

[22] Esfandiari N, Ghoreishi SM. Kinetic Modeling of the Gas Antisolvent Process for Synthesis of 5-Fluorouracil Nanoparticles. Chemical Engineering & Technology. 2014 Jan;37(1):73-80.

[23] Esfandiari N, Ghoreishi SM. Kinetics modeling of ampicillin nanoparticles synthesis via supercritical gas antisolvent process. The Journal of Supercritical Fluids. 2013 Sep 1;81:119-27.

[24] Esfandiari N, Ghoreishi SM. Synthesis of 5-fluorouracil nanoparticles via supercritical gas antisolvent process. The Journal of Supercritical Fluids. 2013 Dec 1;84:205-10.

[25] Jafari D, Nowee SM, Noie SH. A kinetic modeling of particle formation by gas antisolvent process: Precipitation of aspirin. Journal of Dispersion Science and Technology. 2017 May 4;38(5):677-85.

[26] Chen K, Zhang X, Pan J, Zhang W, Yin W. Gas antisolvent precipitation of Ginkgo ginkgolides with supercritical $CO_2$. Powder technology. 2005 Apr 29;152(1-3):127-32.

[27] Bakhbakhi Y, Charpentier PA, Rohani S. Experimental study of the GAS process for producing microparticles of beclomethasone-17, 21-dipropionate suitable for pulmonary delivery. International journal of pharmaceutics. 2006 Feb 17;309(1-2):71-80.

[28] Esfandiari N, Ghoreishi SM. Ampicillin Nanoparticles Production via Supercritical $CO_2$ Gas Antisolvent Process. AAPS PharmSciTech. 2015 Dec 1;16(6):1263-9.

[29] Mukhopadhyay M. Partial molar volume reduction of solvent for solute crystallization using carbon dioxide as antisolvent. The Journal of supercritical fluids. 2003 Apr 1;25(3):213-23.

[30] Kordikowski A, Schenk AP, Van Nielen RM, Peters CJ. Volume expansions and vapor-liquid equilibria of binary mixtures of a variety of polar solvents and certain near-critical solvents. The Journal of Supercritical Fluids. 1995 Sep 1;8(3):205-16.

[31] Esfandiari N, Ghoreishi SM. Optimal thermodynamic conditions for ternary system ($CO_2$, DMSO, ampicillin) in supercritical $CO_2$ antisolvent process. Journal of the Taiwan Institute of Chemical Engineers. 2015 May 1;50:31-6.

[32] Kloc AP, Grilla E, Capeletto CA, Papadaki M, Corazza ML. Phase equilibrium measurements and thermodynamic modeling of {$CO_2$+ diethyl succinate+ cosolvent} systems. Fluid Phase Equilibria. 2019 Dec 15;502:112285.

[33] Su CS, Tang M, Chen YP. Recrystallization of pharmaceuticals using the batch supercritical anti-solvent process. Chemical Engineering and Processing: Process Intensification. 2009 Jan 1;48(1):92-100.

[34] Almeida HM, Marques HM. Physicochemical characterization of finasteride: PEG 6000 and finasteride: Kollidon K25 solid dispersions, and finasteride: β-cyclodextrin inclusion complexes. Journal of Inclusion Phenomena and Macrocyclic Chemistry. 2011 Aug 1;70(3-4):397-406.

[35] Ahmed TA, Al-Abd AM. Effect of finasteride particle size reduction on its pharmacokinetic, tissue distribution and cellular permeation. Drug Delivery. 2018 Jan 1;25(1):555-63.

[36] Yamini Y, Kalantarian P, Hojjati M, Esrafily A, Moradi M, Vatanara A, Harrian I. Solubilities of flutamide, dutasteride, and finasteride as antiandrogenic agents, in supercritical carbon dioxide: Measurement and correlation. Journal of Chemical & Engineering Data. 2010 Feb 11;55(2):1056-9.

[37] Shariati A, Peters CJ. Measurements and modeling of the phase behavior of ternary systems of interest for the GAS process: I. The system carbon dioxide+ 1-propanol+ salicylic acid. The Journal of supercritical fluids. 2002 Aug 1;23(3):195-208.

[38] Bakhbakhi Y, Rohani S, Charpentier PA. Micronization of phenanthrene using the gas antisolvent process. 1. Experimental study and use of FTIR. Industrial & engineering chemistry research. 2005 Sep 14;44(19):7337-44.

[39] De la Fuente Badilla JC, Peters CJ, de Swaan Arons J. Volume expansion in relation to the gas–antisolvent process. The Journal of Supercritical Fluids. 2000 Feb 29;17(1):13-23.

[40] Juan C, Shariati A, Peters CJ. On the selection of optimum thermodynamic conditions for the GAS process. The Journal of supercritical fluids. 2004 Dec 1;32(1-3):55-61.

[41] Peng DY, Robinson DB. A new two-constant equation of state. Industrial & Engineering Chemistry Fundamentals. 1976 Feb;15(1):59-64.

[42] Sodeifian G, Sajadian SA, Ardestani NS. Evaluation of the response surface and hybrid artificial neural network-genetic algorithm methodologies to determine extraction yield of Ferulago angulata through supercritical fluid. Journal of the Taiwan Institute of Chemical Engineers. 2016 Mar 1;60:165-73.

[43] Sodeifian G, Sajadian SA, Ardestani NS. Optimization of essential oil extraction from Launaea acanthodes Boiss: Utilization of supercritical carbon dioxide and cosolvent. The Journal of Supercritical Fluids. 2016 Oct 1;116:46-56..

[44] Wager TD, Nichols TE. Optimization of experimental design in fMRI: a general framework using a genetic algorithm. Neuroimage. 2003 Feb 1;18(2):293-309.

[45] Smit B, Karaborni S, Siepmann JI. Computer simulations of vapor–liquid phase equilibria of n-alkanes. The Journal of chemical physics. 1995 Feb 1;102(5):2126-40.

[46] Reid RC, Prausnitz JM, Poling BE. The properties of gases and liquids.

[47] Marrero J, Gani R. Group-contribution based estimation of pure component properties. Fluid Phase Equilibria. 2001 Jul 1;183:183-208.

[48] Esfandiari N, Estimation of Thermodynamic Properties of Ampicillin and Paclitaxel via Group Contribution, The 9th International Chemical Engineering Congress & Exhibition, Shiraz, Iran, 26-28 December, 2015.

[49] Sajeesh S, Sharma CP. Interpolymer complex microparticles based on polymethacrylic acid-chitosan for oral insulin delivery. Journal of applied polymer science. 2006;99(2):506-12.

[50] Mukhopadhyay M, Dalvi SV. Partial molar volume fraction of solvent in binary ($CO_2$–solvent) solution for solid solubility predictions. The Journal of supercritical fluids. 2004 May 1;29(3):221-30.